Suez Canal Engineering Energy and Environmental Science Journal
Faculty of Engineering – Suez Canal University
2025, Volume. 3, NO. 3 , pages 1– 11

Analytical study on RC Exterior Beam–Column Joints Strengthened with Fiber Sheets under Cyclic Loads

Qais M. Al-Gabri[1]*, Ehab M. lotfy [2], Khaled S. Ragab[3], Manar A. Ahmed[3,4], Abdel- Rahman M. Naguib[2]

[1]Civil Engineering Department, Faculty of Engineering, University of Thamar, Yemen.
[2]Civil Engineering Department, Faculty of Engineering, University of Suez Canal, Egypt.
[3]Reinforced Concrete Research Institute, Housing and Building National Research Center, Egypt.
[4]Faculty of Engineering- Taibah University, Saudi Arabia.

**Corresponding author: Qais Mahdi Al-Gabri, Email address: qaisaljabri503@gmail.com*
DOI: 10.21608/sceee.2025.354773.1062

Article Info:

Article History:
Received: 19\03\2025
Accepted: 20\04\2025
Published: 30\07\2025

DOI: 10.21608/sceee.2025.354773.1062,

Abstract

In this search, a new pattern is suggested to calculate the shear capacity of reinforced concrete (RC) exterior beam-column joints strengthened with fiber-reinforced polymer (FRP) under cyclic loads. A clear formula is developed that accounts for the shear capacity contributions from the transverse reinforcement, main reinforcing bars of the column or beam, and FRP sheet types. The coefficients of each commitment are calibrated utilizing 30 tests in the literature review and 6 experimental tests that had the information needed to derive a new equation. This search compared the inferred equation of Bousselham's model and the modern equation with shear stress of the exterior beam-column joints and found that the values are close to reality when using the modern equation. The proposed method simplifies and ensures the reliability of calculating the necessary FRP sheet enhancements to prevent shear failure in exterior beam-column joints, making it highly useful for researchers and field engineers focused on structures strengthened with FRP sheets under seismic loads.

Keywords: *shear -strength, FRP sheets, Exterior Beam–Column Joints, Reinforced Concrete, Analytical Model.*

Suez Canal Engineering, Energy and Environmental Science Journal (2025), ***vol.3***, No.3.

1. Introduction

Engineers are always looking for new and affordable building materials as well as innovative methods and systems to solve problems. In recent years, research has confirmed that fiber-reinforced polymer (FRP) panels can be effectively used to strengthen concrete elements. FRP is reinforced with high-strength fibers such as carbon fiber-reinforced polymer, aramid fiber-reinforced polymer, glass fiber-reinforced polymer, and hybrids embedded in polymer matrices and is produced in the form of meshes, tubes, and rods in a variety of shapes (Al-Rousan & Alkhawaldeh, 2021). Creating a standardized and universal analytical model or technique to evaluate the behavior of reinforced beam-column connections across various optimization schemes remains a complex challenge. Existing analytical models for these connections often

How to Cite this Article:
Qais M. Al-Gabri. et al. (2025). Analytical study on RC Exterior Beam–Column Joints Strengthened with Fiber Sheets under Cyclic Loads.

vary in terms of reinforcement methods and materials. The primary goal across all models is to assess the extent to which the shear strength of the beam-column connection improves due to joint confinement achieved through reinforcement techniques (Okahashi & Pantelides, 2017). In most of these models, the joint's shear strength serves as a key indicator for evaluating the effectiveness of the applied reinforcement approach. Shear failure is often catastrophic and typically happens without prior warning, making it preferable for beams to fail in flexure rather than shear. Many reinforced concrete (RC) members have been identified as lacking sufficient shear strength and require repair. These deficiencies can arise from several factors, such as inadequate shear reinforcement, loss of steel area due to corrosion, increased service loads, or construction defects. In such cases, externally bonded reinforcements, like FRP sheets, offer an effective solution (Sapidis et al, 2024).

One effective technique for rehabilitating structures damaged by earthquakes involves repair and retrofitting methods. Research indicates that Fiber Reinforced Polymers (FRP) are particularly suitable for retrofitting exterior, interior joints. This is due to their ease of application, cost-efficiency, high resistance to corrosion, low weight, exceptional tensile strength-to-stiffness ratio, and impressive fatigue performance (Marimuthu & Sivasankara, 2021) In many designs, column and beam sizes may be defined by joint design requirements. Careful attention is given to joints to ensure proper structural performance under all reasonably anticipated loading conditions and to alert the designer to the possibility of reinforcement congestion (ACI Committee 352R-2, 2002). Strengthening or retrofitting existing concrete structures to withstand higher design loads, to correct strength loss due to deterioration, to correct design or construction deficiencies, or to improve ductility has traditionally been accomplished using conventional materials and construction techniques The FRP exterior bonding method is conventional construction methods (ACI Committee 440.2R-08, 2008).

Maximum beam-column joint shear strength can be evaluated either using codes like formulations or experimental samples, Codes like formulations represents joint shear strength in terms of concrete main shear strength, with FRP sheets. The predictions generated by these formulas tend to be conservative and often result in underestimations. Empirical and semi-empirical models commonly utilize mechanical methodologies to characterize the force transfer within the joint region. Although the complexity of these models can be substantial, they demonstrate a relatively high degree of accuracy, as they are routinely validated through experimental results, typically showing strong concordance. Nevertheless, over the past two decades, numerous models have been introduced to estimate the shear strength of beam-column joints (Mahmoud, 2018). Externally bonded FRP sheet was renowned as a perfect method as it can eliminate some important restrictions of other traditional strengthening methods (Hadi & Tran, 2014).

In the search, computed equation to estimate effective FRP sheet strain, FRP sheet contribution to main tensile stress and the shear strength increase of exterior joints. Based on a prolonged group of experimental results, distributing by the exterior joint mechanical properties, failure modes and FRP strengthening shapes and design of an improved analytical model.

2. Database of tested external joints

A summary of the main experimental findings and analytical modelling of all available studies was compiled to beam-column joints, containing a total of 30 tests carried out worldwide and Table 1 provides an overview of this created database. The database contains all relevant data, including member dimensions, FRP retrofitting qualities, experimentally measured parameters, the average of the maximal load in the cyclic load, and the mechanical properties of the materials utilized. Concrete with compressive strengths (f_c) ranging between 13.5 and 39.5 MPa was utilized. The subassemblies undergo cyclic testing with axial load ratios in the range $v=N/(A_{col.}f_c)$ = 0.038-0.20 and are distinguished by different member diameters, b_c, h_c, b_b and h_b. The FRP strengthening include: CFRP or GFRP with elastic modulus (E_f) in the range 70–390 GPa, box or strips sheets with directions (0°, 90° or ±45°), thickness of FRP reinforcement, (t_f) ranging 0.053 -1.35 mm; number of layers (n_l) ranging 1 - 3; FRP laminates applied on 1 or 2 sides (n_s) of the joint. The experimental data have been used to derive the joint shear stress at the peak strength v_{jh}^{exp} the slope of the principal compressive stress θ^{exp}, and the FRP equal area, A_{feq}.

These data are required to calculate the effective FRP strain $\varepsilon_{f,e}^{exp}$ and the explained in the last column of Table 1. All specimens failed by joint strength crossed over by or combined with FRP debonding or FRP rupture. Other failure mechanisms that were include beam failure, column failure or hinge, and bond-slip. (Bousselham, 2010) suggested approach to compute the shear strength increase provided by FRP sheet systems, it considers the contribution of the FRP fibers to the principal tensile stress, inclined of 0^O-90^O. Because of the stiffness in the axial direction, the contribution of the FRP sheet can be assumed to be equivalent to the component of the FRP axial stress in the direction of the principal tensile stress in the joint. This model also accounts for the elastic modulus (E_f), of different types of FRP (CFRP, or GFRP), the amount of FRP on the joint (ρ_f) and the substrate mechanical properties (f_c) and predicting the experimental joint shear strain (Bousselham, 2010). The comparison between the predicted FRP strains with those related to increase experimental database (experimental data used by Bousselham, 2010) shows that FRP performances are, in most cases, significantly underestimated; this is because of the FRP strain limitation at 0.004, as shown Fig. 1. Such disregard led to reduce the potential benefits provided by the FRP in strengthening the joint shear capacity.

Table 1. Experimental database on seismic reinforced concrete beam-column joints strengthened with FRP sheets (Source:Literature review with Experimental results).

Subassembly characteristics				Member dimensions				FRP strengthening properties							Parameters Determined Experimental			
Reference	*Specimen ID*	*fc (Mpa)*	*N (KN)*	h_b *(mm)*	b_b *(mm)*	h_c *(mm)*	*bc (mm)*	*Fibers (0)*	E_f *(Gpa)*	*β (0)*	*tf (mm)*	*nl*	*ns*	*FRP shape*	v_{jh}^{exp} *(kN)*	θ^{exp} *(°)*	$A_{f,eq}$ *(mm^2)*	$\varepsilon_{f,e}^{exp}$
(Okahashi & Pantelides, 2017)	STM	34.4	708	610	406	406	406	CFRP	43	±60	1.35	2	2	agonal stri	6.24	56.35	1096.2	0.0169
(De Risi et al., 2020)	NS-FL	25.76	290	500	300	300	300	CFRP	235	0- 90	0.166	1	1	U-strips	3.67	59..03	210.28	0.00923
(De Risi et al., 2020)	NS-FLE	25.76	290	500	300	300	300	CFRP	200	0- 90	0.266	1	1	U- strips	7.73	59.03	336.96	0.0147
(Faleschini et al., 2019)	Sp. 2 – FRP2	39.5	400	500	300	300	300	CFRP	390	0-45 - 90	0.165	2	2	agonal stri	4.86	59.04	835.64	0.0027
(Faleschini et al., 2019)	Sp. 3 – FRP3	39.5	400	500	300	300	300	CFRP	390	0- 90	0.165	2	2	strips, box	4.56	59.04	101.86	0.0023
(Del Vecchio et al., 2015)	T-FL1	13.5	243	500	300	300	300	CFRP	230	0-±45 - 90	0.053	1	1	U-shaped	3.15	56.6	68	0.0047
(Del Vecchio et al., 2015)	T-FS1	17.7	319	500	300	300	300	CFRP	230	0-±45 - 90	0.053	1	1	U-shaped	3.53	58.3	67	0.0047
(Del Vecchio et al., 2015)	T-FS2	16.4	295	500	300	300	300	CFRP	230	0-±45 - 90	0.053	2	1	U-shaped	3.63	57.1	135.14	0.0047
(Zamani Beydokhti et al., 2016)	NS1R	31.12	70	300	300	400	300	CFRP	240	0 - 90	0.167	3	2	- U Shape	5.53	36.87	322.2	0.0149
(Zamani Beydokhti et al., 2016)	NS2R	30.88	70	300	300	400	300	CFRP	240	0 - 90	0.167	3	2	- U Shape	5.23	36.87	322.2	0.0142
(Zamani Beydokhti et al., 2016)	NS3R	30.88	70	300	300	400	300	CFRP	240	0 - 90	0.167	4	2	- U Shape	6.78	36.87	642.84	0.0148
(Zamani Beydokhti et al., 2016)	NS5R	30.8	70	300	300	400	300	CFRP	240	0 - 90	0.167	4	2	- U Shape	6.64	36.87	642.84	0.0148
(Antonopoulos & Triantafillou, 2003)	S33	26	46	300	200	200	200	CFRP	150	0- 90	1.05	1	2	U- strips	3.17	50.1	68	0.006
(Antonopoulos & Triantafillou, 2003)	S63	24.2	46	300	200	200	200	CFRP	150	0- 90	1.05	1	2	U- strips	3.62	49.5	158	0.0037
(Antonopoulos & Triantafillou, 2003)	S33L	26.3	46	300	200	200	200	CFRP	150	0- 90	1.05	1	2	U- strips	4.01	49.1	68	0.0069
(Antonopoulos & Triantafillou, 2003)	F11	22.8	46	300	200	200	200	CFRP	230	0- 90	0.13	1	2	C	3.85	49.3	93	0.0048
(Antonopoulos & Triantafillou, 2003)	F22	27.2	46	300	200	200	200	CFRP	230	0- 90	0.13	2	2	C	4.5	48.6	186	0.0031
(Antonopoulos & Triantafillou, 2003)	(F21	27	46	300	200	200	200	CFRP	230	0- 90	0.13	2	2	C	4.6	48.6	151	0.0039
(Antonopoulos & Triantafillou, 2003)	(F12	29.5	46	300	200	200	200	CFRP	230	0- 90	0.13	1	2	C	4	49.1	127	0.0034
(Antonopoulos & Triantafillou, 2003)	F22A	27.8	115	300	200	200	200	CFRP	230	0- 90	0.13	2	2	C	5.16	52.8	187	0.0028
(Antonopoulos & Triantafillou, 2003)	F22W	29.2	46	300	200	200	200	CFRP	230	0- 90	0.13	2	2	M- C	5.02	48.3	186	0.0024
(Antonopoulos & Triantafillou, 2003)	F22in	21	46	300	200	200	200	CFRP	230	0- 90	0.13	2	2	I - C	3.77	49.3	186	0.0029
(Antonopoulos & Triantafillou, 2003)	GL	19.5	46	300	200	200	200	CFRP	70	0- 90	0.17	2.5	2	C	3.97	49.1	304	0.0054
(Antonopoulos & Triantafillou, 2003)	S-F22	19	46	300	200	200	200	CFRP	230	0- 90	0.13	2	2	C	3.97	49.1	186	0.0027
(Antonopoulos & Triantafillou, 2003)	T-F33	26	46	300	200	200	200	CFRP	230	0- 90	0.13	3	1	C	4	49.1	140	0.0033
(Antonopoulos & Triantafillou, 2003)	T-F22S2	22	46	300	200	200	200	CFRP	230	0- 90	0.13	2	1	2 S	3.6	49.5	93	0.0048
(Allam et al., 2019)	AR-2	34.5	356	406	254	254	254	CFRP	140.7	±45	0.56	2	2	I - C	4.32	55.9	1627	0.0011
(Allam et al., 2019)	RS-SC	34.5	356	406	254	254	254	CFRP	140.7	0- 90 - ±45	0.56	8	2	C	9.75	50.03	8444	0.0012
(Allam et al., 2019)	RS-G	34.5	356	406	254	254	254	GFRP	26.2	0- 90 - ±45	0.1	10	2	C	8.99	50.44	2004	-
(Allam et al., 2019)	RS-MC	34.5	356	406	254	254	254	CFRP	200	0- 90 - ±45	0.8	6	2	C	7.87	51.19	9300	0.0005
Experimental	BCJ6	30	55	200	100	230	100	CFRP	230	0- 90	0.17	1	2	strips	3.45	41	103.21	0.0052
Experimental	BCJ7	30	55	200	100	230	100	CFRP	230	0- 90	0.17	1	2	strips	3.97	41.3	104.09	0.0056
Experimental	BCJ8	30	55	200	100	230	100	GFRP	74	0 - 90	0.17	1	2	strips	3.42	42.1	105.39	0.0045
Experimental	BCJ9	30	55	200	100	230	100	GFRP	74	0 - 90	0.17	1	2	strips	3.52	42.01	105.22	0.0047
Experimental	BCJ10	30	55	200	100	230	100	HFRP	125	0- 90	0.34	1	2	strips	4.2	42.5	106.07	0.0071
Experimental	BCJ11	30	55	200	100	230	100	HFRP	125	0 - 90	0.34	1	2	strips	4.58	42.7	106.41	0.0072

S = Strips, I = Initial damage, M = Mechanical anchorage,C= Continuous fabric.

How to Cite this Article:
Qais M. Al-Gabri. et al. (2025). Analytical study on RC Exterior Beam–Column Joints Strengthened with Fiber Sheets under Cyclic Loads. *Suez Canal Engineering, Energy and Environmental Science Journal*, Volume 3, NO. 3 , pages 1-11

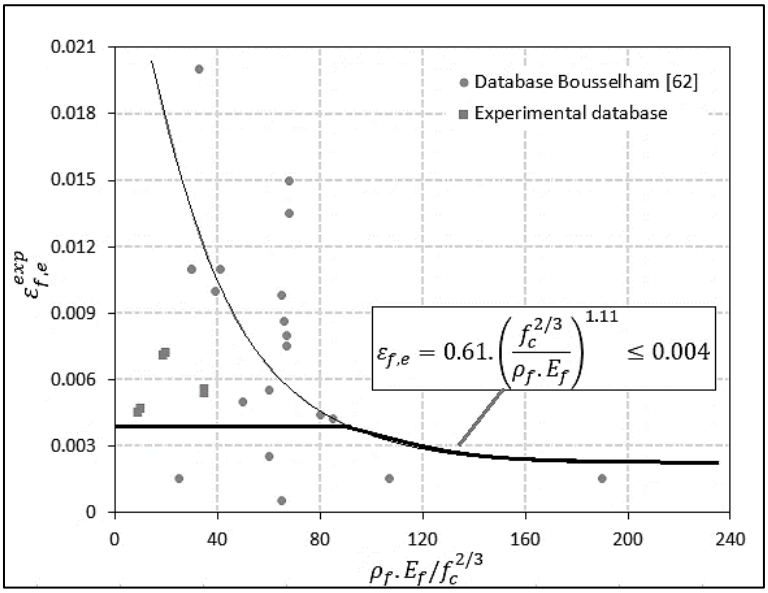

Figure 1: Effective FRP strains beam-column joint: comparison of the experimental data with (Bousselham, 2010) model.

3. Shear strength of the beam-column joint

The horizontal shear stress (v_{jh}^{exp}) at mid-depth of the joint core can be written as:

$$v_{jh}^{exp} = V_{jh}/b_j h_c \qquad (1)$$

where b_j =effective width of the joint core, taken hereafter as the minimum out-of-plane dimension of the beam or column and h_c =depth of the column, as show Fig. 2.

It is possible to compute the joint shear force ($V_{jh,\ \text{retrofitted}}$) for the *FRP* retrofitted specimens by assuming that the tensile force in the longitudinal reinforcement of the beam (T_b) remains constant in the retrofitted specimens. The vertical shear force (V_b) of the beam has been taken as the experimental ultimate load for calculating the maximum horizontal shear force from the experimental investigation (V_{jh}), and the horizontal shear force (V_c) in the column is computed from equation (4). (V_{jh}) retrofitted is determined using equation (2).

$$V_{jh,retrofitted} = T_b + T_{FRP} - V_c \qquad (2)$$

And $T_{FRP} = \mathcal{E}_{FRP} * A_{FRP} * E_{FRP}$

Equation (3) can be used to calculate the design ultimate shear capacity of the joint before failure (V_n), based on theoretical and experimental research (American Concrete Institute ACI 2002).

$$V_n = V_c + V_s, \text{ and } V_s = \frac{f_y.A_S}{\gamma_s}\ , \gamma_s = 1.15 \qquad (3)$$

Where V_c = shear of the concrete, V_s = link shear force strength, f_y = yield strength of the steel bars, A_s = area of the tension steel bars. Using equation (4), the shear capacity of the retrofitted beam-column joints ($V_{n,\ retrofitted}$) can be determined as follows:

$$V_{n,\ retrofitted} = V_c + V_s + V_{FRP} \text{ and}$$
$$V_{FRP} = 0.9\ \mathcal{E}_{FRP} * E_{FRP} * \rho_{FRP} * A_j \qquad (4)$$

Where V_{FRP} = shear force strength of *FRP* reinforced in a joint, ρ_{FRP} is the FRP reinforcement ratio, $\mathcal{E}_{FRP}$ = strain in *FRP* reinforcement, E_{FRP} is the tensile modulus of elasticity, A_j = area of the *FRP* sheets.

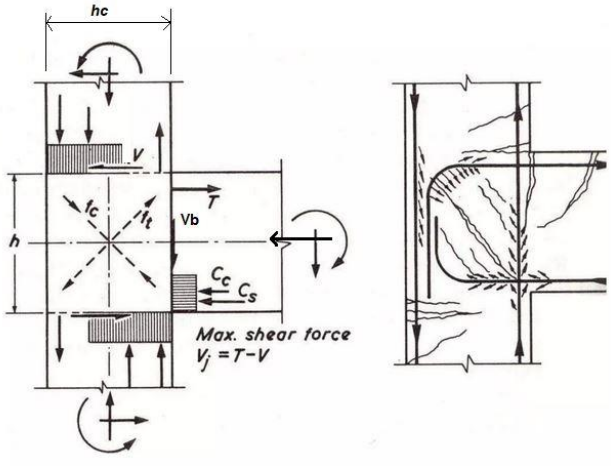

Figure 2: Forces acting in joints under seismic effects (Paulay & Scarpas, 1981)

4. Effective FRP strain of exterior joints

First, the existing experimental information is used to derive the experimental effective FRP strain. Secondly, the power-type equation is obtained by considering the concrete strength, FRP fiber area, and elastic modulus. The shear strength of the FRP-strengthened joints is then calculated using a similar equation, and it is compared to the shear strength of the joints that was obtained through experimentation. Equation of effective FRP strain can be computed by equating the experimentally determined main tensile stress:

$$\varepsilon_{f,e}^{exp} = \frac{p_{t,f}^{exp}.b_c.h_c}{A_{f,eq}.E_f.sin\theta} \qquad (5)$$

Account of parameters of Equation (5):

a) principal tensile stress as measured experimentally ($p_{t,f}^{exp}$) equals:

$$p_{t,f}^{exp} = \left(P_{t,tot}^{exp}\right) - (p_{c,t}) \qquad (6)$$

Where $p_{t,f}^{exp}$ is the total principal tensile stress of the exterior beam-column joints strengthened with FRP sheets, and $p_{c,t}$ refers to an increase in the principal tensile stress of the joint due to concrete. From Mohr's circle analysis, the principal tensile stress at the mid-depth of the joint core ($p_t = p_{t,tot}^{exp}$)is given by:

$$p_t^{exp} = \frac{-\sigma_c}{2}.\sqrt{(\frac{-\sigma_c}{2})^2 + {v_{jh}}^2} \qquad (7)$$

or compression Eq. (8) to values proportional to the compressive strength of concrete.

$$p_c^{exp} = \frac{\sigma_c}{2}.\sqrt{(\frac{\sigma_c}{2})^2 + {v_{jh}}^2} \ \leq 0.5f_c' \qquad (8)$$

From which

$$v_{jh}^{exp} = p_t^{exp}.\sqrt{1 + \frac{\sigma_c}{p_t^{exp}}} \qquad (9)$$

where σ_c =the nominal axial compressive stress on the column at the mid-depth of the joint core, given by:

$$\sigma_c = \frac{N}{b_j h_c} \qquad (10)$$

where N = axial compressive load on the column.

As for exterior joint, in which beam bars bent down across the back of the joint, higher main tension stresses are expected (Bousselham, 2010)

$$p_{t,tot}^{exp} = 0.42\sqrt{f_c'} \qquad (11)$$

The ACI Committee 352-02 provisions (American Concrete Institute ACI, 2002), for instance, states:

$$v_{jh}^{exp} \leq \gamma . \sqrt{f_c'} \qquad (12)$$

where γ empirical constant reflecting confinement of joint by the adjoining members.

Contribution of concrete in principle tensile stress for the deformed bar, exterior beam-column joint is given by:

$$p_{c,t} = k . \sqrt{f_c} \qquad (13)$$

Numerical coefficient (k) = 0.29 when deformed bars are used (at first cracking in joint) or 0.42 (at the maximum strength). The uniform shear stresses (v_{jh}^{exp}) and axial stresses($\sigma_c = f_a$), given by:

$$v_{jh}^{exp} = \frac{V_{jh}}{A_{col.}} \qquad (14)$$

$$\sigma_c = f_a = \frac{N}{A_{col.}} \qquad (15)$$

b) The Mohr's circle approach, the principal compressive stress direction,θ, can be computed:

$$\theta = const = tan^{-1}(\frac{h_b}{h_c}) \qquad (16)$$

c) Equivalent area of FRP, $A_{f,eq}$:

The equal area of the FRP ($A_{f,eq}$) is calculated using the equations for the most common applications of FRP. Uniaxial fabric with fibers in the direction of beam axis (0°) or column axis (90°), see Fig. 3:

$$\begin{cases} A_{f,eq} = n_l \cdot n_s \cdot t_f \cdot h_b \cdot \sin\theta & \text{for} \quad \beta = 0^\circ \\ A_{f,eq} = n_l \cdot n_s \cdot t_f \cdot h_c \cdot \cos\theta & \text{for} \quad \beta = 90^\circ \end{cases} \qquad (14)$$

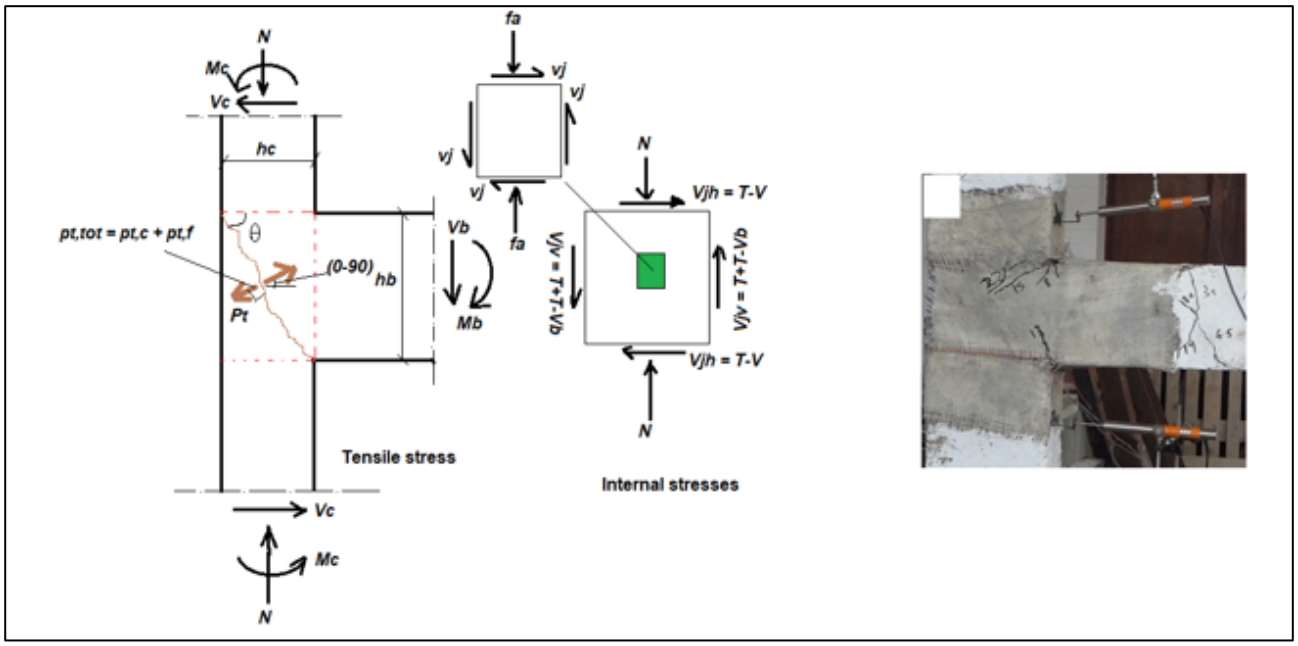

Figure 3: Shear forces of the exterior joint result by cyclic loads (Source: The Researcher)

5. Drawing a curve of the effective FRP strain

There were only 30 tests that had the information needed to derive an equation and 6 experimental tests. Table 1 provides a quick overview of this constructed database. Fig. 4 shows the plot of the effective FRP strain, which is calculated using experimental data on the Y-axis and the constant direction of the primary compressive stress, as a product of the term $A_{f,eq}E_f/f_c^{2/3}$ on the X-axis.

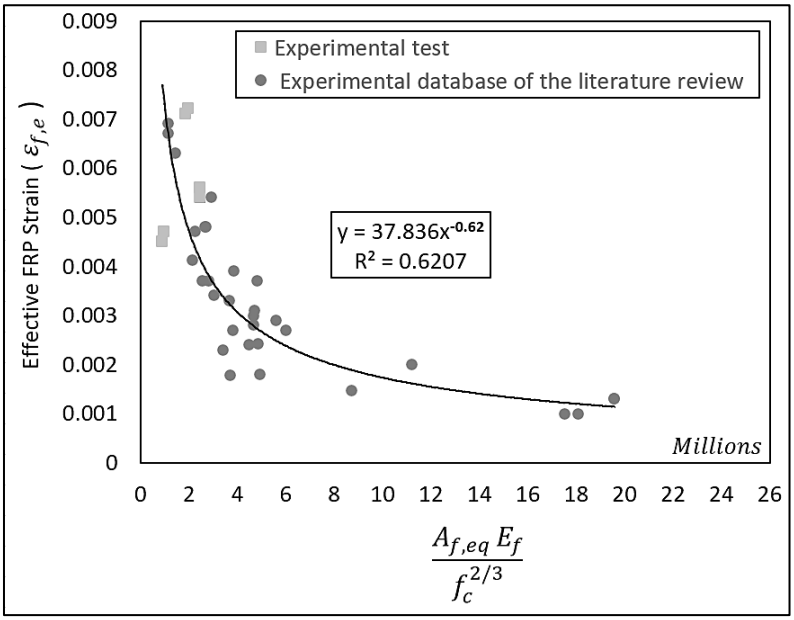

Figure 4: Effective FRP strains for beam-column joint in terms of $A_{f,eq}E_f/f_c^{2/3}$ (Source: The Researcher)

In Fig.3 a power-type expression is employed as the best fit to the data. The final formula for the FRP effective strain is shown in Eq. (15) and includes the two numerical coefficients selected to account for the influence of the mechanical anchorages and initial damage.

$$\varepsilon_{f,e} = 37.83\ x\ k\ x\ m\ x \left(\frac{f_c^{2/3}}{A_{f,eq}.E_f}\right)^{0.62} \qquad (15)$$

If the FRP strengthening system is applied to cracked joint, we use $k_{.}$ = 0.8; otherwise, it is 1.0 in the case of undamaged joint. If the joint FRP strengthening is mechanically anchored at the ends, the coefficient $m_{.}$ = 1.5; otherwise, it is 1.0 if the FRP fibers are extended on the neighboring beams or columns without mechanical anchorages. The effectiveness of the $A_{f,eq}E_f/f_c^{2/3}$ relationship is demonstrated by the strong statistical correlation (R^2 = 0.76) between the data and the variables chosen for the regression.

Design approach, step by step proceedings:

1- Shear strength of the as joint $v_{jh} = p_{t,c}.\sqrt{1+\frac{N/(h_c.b_c)}{p_{t,c}}}$

2- Define the target shear strength, v_{jh}^d (e.g. flexural yielding of beam or column).

3- Select the FRP layout (i.e. continuous fabric, strips, fabric directions, type of fiber, mechanical anchors, and initial damage) and a tentative number of layers (n_l).

4- Calculate the equivalent FRP area $A_{f,eq} = n_l.n_s.t_f.h_c.cos\theta$, assuming $\theta = tan^{-1}(\frac{h_b}{h_c})$.

5- Calculate the effective FRP strain

$$\varepsilon_{f,e} = 37.83\ x\ k\ x\ m\ x \left(\frac{f_c^{2/3}}{A_{f,eq}.E_f}\right)^{0.62}$$

6- Calculate the FRP contribution to the principal tensile stress

$$p_{t,f} = \frac{A_{f,eq}.E_f.\varepsilon_{f,e}}{b_c.h_c/sin\theta}$$

7- Calculate increase in the shear strength:

$$v_{jh} = p_{t,tot}.\sqrt{1+\frac{f_a}{p_{t,tot}}}$$

$p_{t,tot} = p_{t,c} + p_{t,f}$, if $v_{jh} \le v_{jh}^{d}$ increase the number of layers (n_l) and go to step 4.

6. Compared of joint shear stress versus shear stress resulting from inferred equation and modern equation

When comparing the inferred equation (Eq. A Bousselham, 2010) and the modern equation (Eq. B) with joint shear stress it was found that the values are close to reality when using the modern equation as shown in Table 2 and Fig. 5.

$$\varepsilon_{f,e} = 0.61 * \left(\frac{f_c^{\frac{2}{3}}}{\rho_f * E_f}\right)^{1.11} \le 0.004 \quad Eq.A\ (Bousselham, 2010)$$

$$\varepsilon_{f,e} = 37.83\ x\ k\ x\ m\ x \left(\frac{f_c^{2/3}}{A_{f,eq}.E_f}\right)^{0.62} \quad Eq.B\ (Modern\ equation)$$

Table 2. Comparison of joint shear stress predicted with the shear stress resulting from Eq. A and Eq. B (Source: The Researcher)

Reference	Specimens	v_{jh}^{exp}	v_{jh} KN (Eq. A)	v_{jh} KN (Eq. B)	$v_{jh} / v_{jh}^{exp.}$ KN (Eq. A)	$v_{jh} / v_{jh}^{exp.}$ KN (Eq. B)
Experimental	BCJ6	3.45	1.92	3.15	0.56	0.91
Experimental	BCJ7	3.97	2.07	4.32	0.52	1.09
Experimental	BCJ8	3.42	1.88	3.11	0.55	0.91
Experimental	BCJ9	3.52	2.7	3.2	0.77	0.91
Experimental	BCJ10	4.2	2.75	3.92	0.65	0.94
Experimental	BCJ11	3.08	2.08	4.87	0.68	1.58

Notes v_{jh}*: Joint shear stress,* v_{jh} *Eq. A: Shear stress resulting for Eq. B,* v_{jh} *Eq. B: Shear stress resulting Eq. B (Modern equation)*

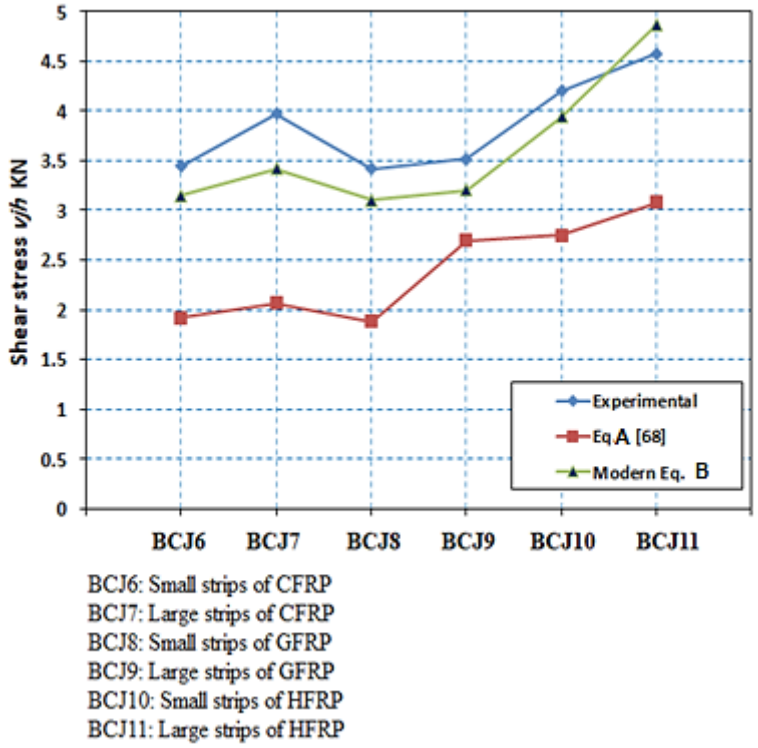

Figure 5: Shear stress resulting from Eq. A and Eq. B and comparison with the experimental value (Source: The Researcher).

7. Conclusions

1. The proposed design procedure is calibrated with experimental tests on exterior joints, using a mechanical properties model of existing structural systems subjected to dangerous seismic behavior. It allows for predicting the shear capacity of exterior joints strengthened with fiber (CFRP, GFRP, and HFRP). This includes different strengthening shapes with a variable number of fibers on the core joint, the quantity of layers, the number of strengthened faces of fibers, continuous strips or reinforcement, and the strengthening system applied to the beam-column joint. Additionally, it involves adopting mechanical stabilization or creating an overlay connection fixed with epoxy to enhance fiber performance. The suggested model enables staff involved in the seismic strengthening of existing structures to readily and reliably quantify the size of FRP reinforcement necessary to prevent the brittle shear failure of beam-column joints.
2. A new general formula was predicted for effective FRP sheet strain, FRP sheet contribution to main tensile stress and the shear strength increase of exterior joints:

$$\varepsilon_{f,e} = 37.83\ x\ k\ x\ m\ x \left(\frac{f_c^{2/3}}{A_{f,eq}.E_f} \right)^{0.62}$$

Nomenclature

Notations	Meaning	Notations	Meaning
V_b	beam shear	M_b	beam bending moment
V_c	column shear	N	column axial load
V_{jh}	horizontal joint shear	n_s	number of joint sides strengthened in shear with FRP systems in the plane of the load
V_{jv}	vertical joint shear	n_l	number of FRP layers
A_{col}	column cross-section area	n_{str}	number of strips on the joint
$A_{f,i}$	FRP area on the joint panel in the generic direction	p_c	joint panel principal compressive stress
$A_{f,eq}$	equivalent FRP area on the joint	p_t	joint panel principal tensile stress
b_c	column width	$P_{t,c}$	concrete contribution to joint principal tensile stress
b_f	width of the FRP sheet	$P_{t,f}$	FRP contribution to joint principal tensile stress
$C_{I.D.}$	numerical coefficient for initial damage	$p_{t,f,i}$	contribution of the FRP fibers in the generic direction to joint panel principal tensile stress
$C_{A.M.}$	numerical coefficient for mechanical anchorage	$P_{t,tot}$	joint panel total principal tensile stress
d_b	beam internal lever arm	T	total tension force in the longitudinal reinforcements
E_f	Young's modulus of FRP fibers	t_f	equivalent thickness of the FRP reinforcement (dry fibers only)
f_a	column axial stress	v_{jh}	horizontal joint shear stress
f_c	mean concrete cylinder compressive strength	w_f	strip width
$f_{f,e}$	FRP effective tensile stress	β	inclination of joint panel FRP fibers
h_b	beam height	β_i	generic direction of FRP fibers
h_c	column height	$\varepsilon_{f,e}$	effective FRP strain
l_b	beam length measured from the column face	v	axial load ratio $[N/(b_c.h_c.f_c)]$
θ	inclination of concrete compressive strut, assumed equal to inclination of joint cracks	ρ_f	FRP area fraction

References

Al-Rousan, R. Z., & Alkhawaldeh, A. Numerical simulation of the influence of bond strength degradation on the behavior of reinforced concrete beam-column joints externally strengthened with FRP sheets. Case Studies in Construction Materials 2021, 15, e00567.

Okahashi, Y., & Pantelides, C. P. Strut-and-tie model for interior RC beam-column joints with substandard details retrofitted with CFRP jackets. Composite Structures 2017, 165, 1-8.

Sapidis, G. M., Naoum, M. C., Papadopoulos, N. A., Golias, E., Karayannis, C. G., & Chalioris, C. E. A Novel Approach to Monitoring the Performance of Carbon-Fiber-Reinforced Polymer Retrofitting in Reinforced Concrete Beam–Column Joints. Applied Sciences 2024, 14(20), 9173.

How to Cite this Article:
Qais M. Al-Gabri. et al. (2025). Analytical study on RC Exterior Beam–Column Joints Strengthened with Fiber Sheets under Cyclic Loads. *Suez Canal Engineering, Energy and Environmental Science Journal,* Volume 3, NO. 3 , pages 1-11

Marimuthu, S., & Sivasankara Pillai, G. Experimental investigation of exterior reinforced concrete beam-column joints strengthened with hybrid FRP laminates. Građevinar 2021, 73(04.), 365-379.

ACI Committee 352R-2. Recommendations for design of beam-column connections in monolithic reinforced concrete structures 2002, June 18.

ACI Committee 440.2R-08. Guide for the design and construction of externally bonded FRP systems for strengthening concrete structures 2008, July.

Mahmoud, A. A. H. Effect of joint details on the behavior of RC beam column connections subjected to reversed cyclic loading. journal of al-azhar university engineering sector 2018, 13(49), 1392-1403.

Hadi, M. N., & Tran, T. M. Retrofitting nonseismically detailed exterior beam–column joints using concrete covers together with CFRP jacket. Construction and Building Materials 2014, 63, 161-173.

Bousselham A. State of research on seismic retrofit of RC beam–column joints with externally bonded FRP. ASCE J Compos Constr 2010; 14:49–61.

Paulay, T., & Scarpas, A. The behavior of exterior beam-column joints. Bulletin of the New Zealand Society for Earthquake Engineering 1981, 14(3), 131-144.

De Risi, M. T., Del Vecchio, C., Ricci, P., Di Ludovico, M., Prota, A., & Verderame, G. M. Light FRP Strengthening of Poorly Detailed Reinforced Concrete Exterior Beam–Column Joints. Journal of Composites for Construction 2020, 24(3), 04020014.

Faleschini, F., Gonzalez-Libreros, J., Zanini, M. A., Hofer, L., Sneed, L., & Pellegrino, C. Repair of severely-damaged RC exterior beam-column joints with FRP and FRCM composites. Composite Structures 2019, 207, 352-363.

Del Vecchio, C., Di Ludovico, M., Prota, A., & Manfredi, G. Analytical model and design approach for FRP strengthening of non-conforming RC corner beam–column joints. Engineering Structures 2015, 87, 8-20.

Zamani Beydokhti, E., & Shariatmadar, H. Strengthening and rehabilitation of exterior RC beam–column joints using carbon-FRP jacketing. Materials and Structures 2016, 49, 5067-5083.

Antonopoulos, C. P., & Triantafillou, T. C. Experimental investigation of FRP-strengthened RC beam-column joints. Journal of composites for construction 2003, 7(1), 39-49.

Allam, K., Mosallam, A. S., & Salama, M. A. Experimental evaluation of seismic performance of interior RC beam-column joints strengthened with FRP composites. Engineering Structures 2019, 196, 109308.